

Coping with Negative Short-Rates

Zura Kakushadze^{§†1}

[§] *Quantigic® Solutions LLC*

*1127 High Ridge Road #135, Stamford, CT 06905*²

[†] *Free University of Tbilisi, Business School & School of Physics*
240, David Agmashenebeli Alley, Tbilisi, 0159, Georgia

(February 9, 2015; revised: August 7, 2015)

Abstract

We discuss a simple extension of the Ho and Lee model with generic time-dependent drift in which: 1) we compute bond prices analytically; 2) the yield curve is sensible and the asymptotic yield is positive; and 3) our analytical solution provides a clean and simple way of separating volatility from the drift in the short-rate process. Our extension amounts to introducing one or two reflecting barriers for the underlying Brownian motion (as opposed to the short-rate), which allows to have more realistic time-dependent drift (as opposed to constant drift). In our model the spectrum – or, roughly, the set of short-rate values contributing to bond and other claim prices – is discrete and positive. We discuss how to calibrate our model using empirical yield data by fitting three parameters and then read off the time-dependent drift.

¹ Zura Kakushadze, Ph.D., is the President of Quantigic® Solutions LLC, and a Full Professor at Free University of Tbilisi. Email: zura@quantigic.com

² DISCLAIMER: This address is used by the corresponding author for no purpose other than to indicate his professional affiliation as is customary in publications. In particular, the contents of this paper are not intended as an investment, legal, tax or any other such advice, and in no way represent views of Quantigic Solutions LLC, the website www.quantigic.com or any of their other affiliates.

1 Introduction

An allure of short-rate models is their apparent elegance and simplicity. In theory, once the short-rate process r_t and the corresponding risk neutral measure are specified, bonds and other claims, such as bond options, can be priced via simple-looking conditional expectations of “exponentially” discounted claims. However, in practice, things are a bit trickier. In their simplest incarnations, *e.g.*, Merton’s (1973) model and the Ho and Lee (1986) model, short-rate models typically³ produce unrealistic yield curves for zero-coupon bonds, with long-maturity yields turning negative.

An immediately evident – but not necessarily relevant – culprit would appear to be that in such models r_t can become negative. However, intuitively, since r_t is not observable in real life, it taking negative values need not be a big deal. Instead, what is important is that the model yield curve be sensible. Thus, in the Vasicek (1977) model r_t can become negative, but for a range of parameters the model yield curve *a priori* appears sensible as the spectrum in this model is discrete and bounded from below. In models such as Merton’s model and the Ho and Lee model the spectrum is continuous and unbounded. Intuitively, the “spectrum” here can be thought of as the set of values of r_t that actually contribute to the bond (and other claim) prices.⁴

While the spectrum in the Vasicek model is bounded from below, it is nonnegative only if, roughly speaking, volatility is low. In some cases, including in the current low interest rate environment with not-so-low volatility, this can be problematic. In fact, one can ensure that r_t is always positive and can never reach zero as, *e.g.*, in the Black and Karasinski (1991) model, where $\ln(r_t)$ is the Vasicek process. However, here too, low interest rates by construction imply low (almost vanishing) volatility.

An alternative approach to ensure $r_t \geq 0$ is to introduce a reflecting barrier at $r_t = 0$, or to treat r_t as an option on an underlying “shadow” rate X_t (which can be negative) by taking its positive part,⁵ as in (Black, 1995) and (Rogers, 1995, 1996). Short-rate models with a reflecting barrier at $r_t = 0$ were studied in (Goldstein and Keirstead, 1997) for Merton’s model, the Vasicek model, the extended (a.k.a. shifted) CIR (Cox, Ingersoll and Ross, 1985) model, and the Longstaff (1989) model. Models with r_t as an option were studied in (Gorovoi and Linetsky, 2004) when the “shadow” rate X_t follows the Vasicek model and the shifted CIR model. In this approach volatility generally need not be small even in the low interest rate regime.

In all the models studied in (Goldstein and Keirstead, 1997) and (Gorovoi and

³ One can circumvent this via apparently unrealistic time dependence for the drift in r_t .

⁴ Mathematically, the “spectrum” is the set of eigenvalues for the static Schrödinger equation to which the pricing PDE reduces, *e.g.*, when the underlying parameters are time-independent.

⁵ For a reflecting barrier at $r_t = 0$ we have a Neumann boundary condition w.r.t. r_t ($r_t \in \mathbf{R}^+$) and the system can be described via $r_t = |X_t|$ with claims symmetric under $X_t \rightarrow -X_t$. The spectrum is discrete and positive even if $X_t \in \mathbf{R}$ follows Merton’s model or the Ho and Lee model (see below). For r_t as an option we have $r_t = (X_t)^+$ (with the “shadow” rate $X_t \in \mathbf{R}$), and at $r_t = 0$ we sew together solutions with $r_t = 0$ ($X_t \in \mathbf{R}^-$) and $r_t = X_t \in \mathbf{R}^+$ by requiring continuity of the claim price and its first derivative w.r.t. X_t . Here the $r_t = X_t \in \mathbf{R}$ model is assumed to have a discrete spectrum, and then the spectrum in the $r_t = (X_t)^+$ model is discrete and positive.

Linetsky, 2004) the underlying parameters (volatility, drift, mean-reversion rate, *etc.*) are assumed to be constant. More generally, in time-homogeneous cases (where the parameters depend on r_t (or X_t) but have no explicit time dependence), we have the standard separation of variables and the pricing PDE reduces to an ODE (static Schrödinger equation). Also, at $r_t = 0$ we have a time-independent boundary condition for a reflective barrier and a time-independent sewing condition for r_t as an option. These nice simplifying features are lost once we consider time-dependent parameters, which in many cases are required to describe real-life yield curves.

However, not all is lost. In this paper we set forth a simple way of circumventing this difficulty. The following observations will pave the way for us. First, to get a sensible yield curve (and, more generally, claim pricing), it is not required that r_t be nonnegative.⁶ What is required is that the spectrum be discrete and nonnegative.⁷ To achieve this, it suffices to introduce a reflecting barrier for the underlying Brownian motion W_t (as opposed to r_t). Then we can have time-dependent drift and still achieve separation of variables. Furthermore, the resulting boundary condition is also time-independent. Second, with a reflecting barrier for W_t , the spectrum is discrete and positive (roughly, if $r_t > r_- < 0$)⁸ already in the Ho and Lee model⁹

$$dr_t = \sigma dW_t + \nu(t) dt \tag{1}$$

where we take constant volatility σ and general time-dependent drift $\nu(t)$ and solve the pricing problem analytically.¹⁰ Because of the simplicity of the diffusion part in the Ho and Lee model, our analytical solution provides a clean and simple way of separating volatility in r_t from the drift. We discuss how to fit this model into an empirical yield curve, which involves calibrating three constant parameters (volatility σ , the initial value of r_t , and the location of the reflecting barrier) and then read off the time-dependent drift, or, equivalently, its contribution to the yield curve. We illustrate our method by fitting the model into recent U.S. Treasury yield data.

The remainder of this paper is organized as follows. In Section 2 we briefly review some generalities of short-rate models and then discuss how to introduce reflecting barriers for short-rate processes of the form $r_t = U(W_t) + \chi(t)$ and solve the claim pricing problem. In Section 3 we apply the results of Section 2 to the Ho and Lee model with one and two reflecting barriers, give explicit formulas for zero-coupon bond prices, and for illustrative and comparison purposes discuss fitting the model into the Japanese Government Bond data used to calibrate a model in (Gorovoi and Linetsky, 2004). We also discuss a fit into recent U.S. Treasury yield data. We briefly conclude in Section 4. Some technical details are relegated to Appendices.

⁶ Thus, the models studied in (Goldstein and Keirstead, 1997) and (Gorovoi and Linetsky, 2004) can have: a reflecting barrier at $r_t = r_- < 0$; and $r_t = r_- + (X_t)^+$ with $r_- < 0$, respectively.

⁷ Realistically, the lowest eigenvalue has to be reasonably positive (see below).

⁸ *I.e.*, for this purpose alone we do not need more complex (Vasicek, CIR, *etc.*) dynamics.

⁹ More generally, we discuss factorized processes of the form $r_t = U(W_t) + \chi(t)$. Furthermore, if desired, we can have $r_t \geq 0$ by appropriately choosing parameters. However, this is not required.

¹⁰ Both for one reflecting barrier (say, at $W_t = 0$) and two reflecting barriers (at $W_t = 0$ and $W_t = L$). The latter case can be useful for preventing r_t from wandering away into large values.

2 Short-rate Models

A short-rate model posits a risk-neutral measure \mathbf{Q} and a short-rate process r_t . The cash bond process is given by

$$B_t = \exp \left(\int_0^t r_s ds \right) \quad (2)$$

while the price at time t of a claim X at maturity T is given by $v(r_t, t, T)$, where the pricing function $v(z, t, T)$ is given by

$$v(z, t, T) \equiv \left\langle \exp \left(- \int_t^T r_s ds \right) X \right\rangle_{\mathbf{Q}, r_t=z} \quad (3)$$

E.g., for $X = 1$, we have $v(r_t, t, T) = P(t, T)$, and $v(z, T, T) = 1$, where $P(t, T)$ is the price of a zero-coupon T -bond. Also, $\langle \cdot \rangle$ denotes expectation.

In short-rate models one usually works with a parameterized family of processes, and chooses the parameters to best fit the market. Thus, typically one *assumes* that r_t satisfies the following SDE:

$$dr_t = \sigma(r_t, t) dW_t + \nu(r_t, t) dt \quad (4)$$

where $\sigma(z, t)$ and $\nu(z, t)$ are deterministic functions, and W_t is a \mathbf{Q} -Brownian motion. The pricing function $v(z, t, T)$ satisfies a pricing PDE¹¹, which follows from the requirement that the discounted process $Z(t, T) \equiv B_t^{-1} v(r_t, t, T)$ be a martingale under the risk-neutral measure \mathbf{Q} :

$$\nu(r_t, t) \partial_z v(r_t, t, T) + \partial_t v(r_t, t, T) + \frac{1}{2} \sigma^2(r_t, t) \partial_z^2 v(r_t, t, T) - r_t v(r_t, t, T) = 0 \quad (5)$$

with the terminal condition $v(z, T, T) = \langle X \rangle_{\mathbf{Q}, r_T=z} \equiv \tilde{Y}(z)$.

2.1 Mean-Reversion and Positivity

In some cases one may wish to require that the short-rate process r_t not wander away to large values. One way to achieve this is to use a mean-reverting process

$$dX_t = \sigma(t) dW_t + [\theta(t) - \alpha(t) r_t] dt \quad (6)$$

where $\sigma(t)$, $\theta(t)$ and $\alpha(t)$ depend only on time. For constant σ , θ and α we have the mean-reverting Ornstein-Uhlenbeck process. In the Vasicek/Hull-White model we have $r_t = X_t$. One “shortcoming” of this model is that r_t can occasionally become negative.¹² One way to deal with this is to consider short-rate models of the form $r_t = r_0 f(X_t)/f(0)$, where $f(y)$ is a positive function, *e.g.*, $f(y) = \exp(y)$, which is the Black-Karasinski model. The path integral treatment of such models was discussed in (Kakushadze, 2014).¹³

¹¹ Known as the Feynman-Kac equation, a.k.a. the Arrow-Debreu security PDE.

¹² More relevantly (see below), *e.g.*, for constant σ , θ and α , the asymptotic (*i.e.*, large T) zero-coupon bond yield in this model is positive only for $\sigma^2 < 2\alpha\theta$.

¹³ The results we obtain below can also be derived using path integral.

2.2 Short-rate Models with Reflecting Barriers

An alternative approach is to consider short-rate processes of the form $r_t = U(W_t, t)$, where the function $U(x, t)$ is bounded. More precisely, here we can consider three cases: i) x is unrestricted, $x \in \mathbf{R}$; ii) x takes values on a half-infinite line, $x \in [x_-, \infty)$ or $x \in (-\infty, x_+]$; and iii) x takes values on a finite interval, $x \in [x_-, x_+]$. In the case iii), $U(x, t)$ can be a simple function, *e.g.*, $U(x, t) = a(t)x + b(t)$, even though it is not bounded when extended to the entire real line $x \in \mathbf{R}$. In the case ii), r_t is nonnegative¹⁴ so long as $U(x, t) \geq 0$ for, say, $x \in [x_-, \infty)$.

In the following we will assume that, for the allowed values of x , for a given value of t , there is a one-to-one mapping between z and x via $z = U(x, t)$. Then the pricing PDE (5) simplifies as follows. Let $\tilde{Y}(U(x, T)) \equiv Y(x)$ and¹⁵ $v(U(x, t), t, T) \equiv \psi(x, t)$. Also, we have $\sigma(r_t, t) = \partial_x U(x, t)$ and $\nu(r_t, t) = \partial_x^2 U(x, t)/2 + \partial_t U(x, t)$, where $U(x, t) = r_t$, and the pricing PDE (5) reads:

$$\partial_t \psi(x, t) = -\frac{1}{2} \partial_x^2 \psi(x, t) + U(x, t) \psi(x, t) \quad (7)$$

$$\psi(x, T) = Y(x) \quad (8)$$

where (8) is the terminal condition at $t = T$. For definiteness, here we focus on the case with two boundaries. Cases with a single (lower or upper) boundary follow upon removing the unwanted boundary to the corresponding infinity and requiring that $\psi(x, t)$ be finite (actually, vanish) at such infinity.

Since we have boundaries, we need to specify boundary conditions. For the reasons which will become evident momentarily, we will take the boundaries x_{\pm} to be reflecting barriers, *i.e.*, when the Brownian motion touches the lower (upper) boundary x_- (x_+) from above (below), it is reflected back into the values $x > x_-$ ($x < x_+$). This implies that we have Neumann boundary conditions

$$\partial_x \psi(x_-, t) = 0 \quad (9)$$

$$\partial_x \psi(x_+, t) = 0 \quad (10)$$

This then implies that $Y(x)$ also satisfies Neumann boundary conditions:

$$\partial_x Y(x_-) = 0 \quad (11)$$

$$\partial_x Y(x_+) = 0 \quad (12)$$

Had we imposed the Dirichlet boundary conditions $\psi(x_-, t) = 0$ and $\psi(x_+, t) = 0$, for which the process W_t is not allowed to touch the boundaries, we would invariably have $Y(x_-) = 0$ and $Y(x_+) = 0$. This would not be suitable for our purposes here

¹⁴ Albeit, as discussed above and below, nonnegativity of r_t is actually no longer required in cases ii) and iii) and is replaced by a weaker condition.

¹⁵ When $U(x, t)$ has no explicit time dependence, we have time translational invariance and $\psi(x, t)$ depends on T only via the combination $T - t$. However, this is no longer the case when $\partial_t U(x, t) \neq 0$. Nonetheless, below we will use the abbreviated notation $\psi(x, t)$.

as Dirichlet boundary conditions are incompatible with, *e.g.*, the claim $X = 1$ for a zero-coupon T -bond.¹⁶

Note that (7) is the Schrödinger equation in imaginary (Euclidean) time for a particle (with mass $m = 1$ and Planck's constant $\hbar = 1$) in the potential $U(x, t)$. For general time-dependent potentials $U(x, t)$ Eq. (7) is difficult to solve. However, for our purposes here it will suffice to consider factorized potentials of the form

$$U(x, t) = V(x) + \chi(t) \quad (13)$$

For such potentials we have $\sigma(r_t, t) = V'(x)$ and $\nu(r_t, t) = V''(x)/2 + \dot{\chi}(t)$, where a prime denotes a derivative w.r.t. x , while a dot stands for a derivative w.r.t. t , and $r_t = V(x) + \chi(t)$.

For the factorized potential (13), we have separation of variables, and the solution to (7) can be written in terms of a series ($E_1 < E_2 < E_3 < \dots$):¹⁷

$$\psi(x, t) = e^{-\eta(t, T)} \sum_{n=1}^{\infty} c_n \psi_n(x) e^{-\chi_n(t)(T-t)} \quad (14)$$

$$\eta(t, T) \equiv \int_t^T ds [\chi(s) - \chi(t)] \quad (15)$$

$$\chi_n(t) \equiv \chi(t) + E_n \quad (16)$$

where $\psi_n(x)$, $n \in \mathbf{N}$ is the complete orthonormal set of solutions to the static Schrödinger equation:

$$-\frac{1}{2} \partial_x^2 \psi_n(x) + V(x) \psi_n(x) = E_n \psi_n(x) \quad (17)$$

$$\int_{x_-}^{x_+} dx \psi_n(x) \psi_{n'}(x) = \delta_{nn'} \quad (18)$$

subject to the Neumann boundary conditions

$$\partial_x \psi_n(x_-) = 0 \quad (19)$$

$$\partial_x \psi_n(x_+) = 0 \quad (20)$$

If we have a single lower (upper) reflecting boundary at x_- (x_+), then we have only one Neumann boundary condition at this boundary together with the requirement that $\psi_n(x)$ vanish as $x \rightarrow +\infty$ ($-\infty$).

For a zero-coupon T -bond we have $X = 1$ and $v(r_t, t, T) = P(t, T)$, where $P(t, T)$ is the bond price. The yield is given by

$$R(t, T) = -\frac{\ln(P(t, T))}{T - t} \quad (21)$$

¹⁶ We could consider inhomogeneous boundary conditions such that $Y(x)$ would not need to satisfy Neumann boundary conditions. However, this will not be needed for our purposes here.

¹⁷ Here we are assuming that the eigenvalue spectrum E_n is discrete and bounded from below. This is the case if the potential $V(x)$ is confining, even without the boundaries. With one or two boundaries, it suffices that $V(x)$ is bounded from below for the allowed range of x .

The asymptotic yield must be nonnegative¹⁸

$$0 \leq R_*(t) \equiv \lim_{T-t \rightarrow +\infty} R(t, T) = \chi_*(t) + \chi_1(t) = \chi_*(t) + \chi(t) + E_1 \quad (22)$$

where

$$\chi_* \equiv \lim_{T-t \rightarrow +\infty} \frac{\eta(t, T)}{T-t} \quad (23)$$

Assuming $\chi_*(t)$ is finite, we have a requirement that $E_1 \geq -\chi_*(t) - \chi(t)$.

The coefficients c_n (for a general claim $Y(x)$) are given by

$$c_n = \int_{x_-}^{x_+} dx \, \psi_n(x) Y(x) \quad (24)$$

which is a consequence of (8) and (18). To recap, the pricing function $v(z, t, T)$ is given by

$$v(z, t, T) = e^{-\eta(t, T)} \sum_{n=1}^{\infty} c_n \psi_n(x) e^{-\chi_n(t)(T-t)} \quad (25)$$

where x is related to z via $V(x) + \chi(t) = z$.

3 Ho and Lee Model with Reflecting Barriers

Let us consider the simplest example, the Ho and Lee model

$$dr_t = \sigma dW_t + \nu(t) dt \quad (26)$$

where σ is constant, but the drift $\nu(t)$ *a priori* is an arbitrary function of t (subject to some restrictions we discuss below). We have

$$r_t = \sigma W_t + \chi(t) \quad (27)$$

where (we are assuming $W_0 = 0$)

$$\chi(t) \equiv r_0 + \int_0^t ds \, \nu(s) \quad (28)$$

So, $V(x) = \sigma x$.

The static Schrödinger equation (17) reads:

$$-\frac{1}{2} \partial_x^2 \psi_n(x) + \sigma x \psi_n(x) = E_n \psi_n(x) \quad (29)$$

The solution depends on the boundary conditions and is expressed via a linear combination of $Ai(\alpha x - e_n)$ and $Bi(\alpha x - e_n)$, where $\alpha \equiv (2\sigma)^{1/3}$, $e_n \equiv E_n/\beta$, $\beta \equiv \sigma/\alpha = (\sigma^2/2)^{1/3}$, and the Airy functions $Ai(y)$ and $Bi(y)$ are the two independent solutions of the Airy equation $f''(y) = y f(y)$.

¹⁸ Realistically, the asymptotic yield should not be less than some positive number.

3.1 Ho and Lee Model on a Semi-infinite Line

Thus, let us consider the Ho and Lee model (26) on a semi-infinite line, *i.e.*, we restrict the values of W_t to \mathbf{R}^+ , where without loss of generality we have set $x_- = 0$. We have (29) with only one Neumann boundary condition

$$\partial_x \psi_n(0) = 0 \quad (30)$$

and the requirement that $\psi_n(x)$ be finite as $x \rightarrow +\infty$. The solution is given by:

$$\psi_n(x) = a_n \text{Ai}(\alpha x - e_n) \quad (31)$$

where

$$e_n = -\xi_n \quad (32)$$

Here ξ_n ($0 > \xi_1 > \xi_2 > \dots$) are the zeros of the first derivative of $\text{Ai}(y)$:

$$\text{Ai}'(\xi_n) = 0 \quad (33)$$

Note that the integration in (24) is from 0 to $+\infty$. The normalization coefficients

$$a_n^{-2} \equiv \int_0^\infty dx [\text{Ai}(\alpha x - e_n)]^2 = -\alpha^{-1} \xi_n [\text{Ai}(\xi_n)]^2 \quad (34)$$

where we have used (70) (see Appendix A).

3.1.1 “Modulus” Ho and Lee Model

In the Ho and Lee model on a semi-infinite line the short-rate process r_t generally is unbounded from above. If this is not problematic,¹⁹ then we do not even need to restrict the process r_t to a semi-infinite line. Instead, we can simply consider a “modulus” model:²⁰

$$r_t = \sigma |W_t| + \chi(t) \quad (35)$$

where W_t is unrestricted. In this case we have

$$\psi_n(x) = a_n \text{Ai}(\alpha x - e_n), \quad x \geq 0 \quad (36)$$

$$\psi_n(x) = (-1)^{n+1} \psi_n(-x), \quad x < 0 \quad (37)$$

$$a_n^{-2} \equiv 2 \int_0^\infty dx [\text{Ai}(\alpha x - e_n)]^2 \quad (38)$$

$$a_n^{-2} = 2 \alpha^{-1} e_n [\text{Ai}(-e_n)]^2, \quad n = 1, 3, \dots \quad (39)$$

$$a_n^{-2} = 2 \alpha^{-1} [\text{Ai}'(-e_n)]^2, \quad n = 2, 4, \dots \quad (40)$$

¹⁹ *E.g.*, for given volatility σ , we are interested in time horizons such that r_t simply does not have enough time to wander away too far.

²⁰ Note the difference with, *e.g.*, an alternative model $r_t = |\sigma W_t + \chi(t)|$. The latter is harder to tackle for general $\chi(t)$. See Appendix B for details.

and e_n are now given by

$$e_n = -\xi_{(n+1)/2}, \quad n = 1, 3, \dots \quad (41)$$

$$e_n = -\zeta_{n/2}, \quad n = 2, 4, \dots \quad (42)$$

Here ζ_n ($0 > \zeta_1 > \zeta_2 > \dots$) are the zeros of $Ai(y)$:

$$Ai(\zeta_n) = 0 \quad (43)$$

Note that the integration in (24) is now from $-\infty$ to $+\infty$.

The solutions $\psi_n(x)$ with odd n are symmetric w.r.t. the \mathbf{Z}_2 reflections $x \rightarrow -x$ and satisfy the Neumann boundary condition (30), while the solutions with even n are antisymmetric and satisfy the Dirichlet boundary condition $\psi_n(0) = 0$. The short-rate process is invariant under $W_t \rightarrow -W_t$, so the claims should also be symmetric: $Y(-x) = Y(x)$. Then we have $c_n = 0$ for even n , and for odd n we have

$$c_n = 2 \int_0^\infty dx \psi_n(x) Y(x) \quad (44)$$

It then follows (taking into account the differing by $\sqrt{2}$ normalizations for $\psi_n(x)$ in the two cases) that, for the same (symmetric) claim $X = Y(W_T)$, the pricing function $v(z, t, T)$ is the same in the Ho and Lee Model on a semi-infinite line and in the “modulus” model (35) – as they should be based on symmetry considerations.

3.2 Ho and Lee Model on an Interval

Assuming the reflecting barriers at $x = 0$ and $x = L$, the Brownian motion W_t wanders between 0 and L . We have (29) with two Neumann boundary conditions

$$\partial_x \psi_n(0) = \partial_x \psi_n(L) = 0 \quad (45)$$

The solution to (29) is given by

$$\psi_n(x) = a_n \phi_n(x) \quad (46)$$

$$\phi_n(x) \equiv Ai(\alpha x - e_n) - Q(0, e_n) Bi(\alpha x - e_n) \quad (47)$$

$$Q(x, e) \equiv \frac{Ai'(\alpha x - e)}{Bi'(\alpha x - e)} \quad (48)$$

where e_n are the roots of the following equation for e :

$$Q(L, e) = Q(0, e) \quad (49)$$

which has an infinite tower of discrete solutions $e_n > 0$, $n \in \mathbf{N}$. The normalization coefficients

$$a_n^{-2} \equiv \int_0^L dx \phi_n^2(x) = \frac{1}{\alpha} [e_n \phi_n^2(0) + (\alpha L - e_n) \phi_n^2(L)] \quad (50)$$

where we have used (49) and (70) (see Appendix A). Note that if we take $L \rightarrow \infty$, (50) reduces to (34), as it should.

3.2.1 “Periodic” Ho and Lee Model

Just as in the case of the Ho and Lee model on a semi-infinite line, the Ho and Lee model on an interval is also equivalent to a model where W_t is unrestricted. In this unbounded model the short-rate process has the following “periodic” form

$$r_t = \sigma h(W_t) + \chi(t) \quad (51)$$

where $h(x)$ is a piecewise linear periodic function

$$h(x) = x, \quad 0 \leq x \leq L \quad (52)$$

$$h(x) = 2L - x, \quad L \leq x \leq 2L \quad (53)$$

$$h(x + 2L) = h(x) \quad (54)$$

and the claim $X = Y(W_T)$ is symmetric under both $x \rightarrow -x$ and $L + x \rightarrow L - x$ reflections: $Y(-x) = Y(x)$ and $Y(L - x) = Y(L + x)$. This implies that $Y(x)$ is periodic: $Y(x + 2L) = Y(x)$. Therefore, the integration in (24) is from 0 to $2L$, or, equivalently, from $-L$ to L .

3.3 Bond Pricing on a Semi-infinite Line

For illustrative purposes, let us discuss zero-coupon T -Bond pricing, for which the claim is simply $X = 1$. For the Ho and Lee model on a semi-infinite line we have

$$c_n = \int_0^\infty dx \psi_n(x) = \frac{1}{\alpha} a_n \int_{\xi_n}^\infty dy Ai(y) = \frac{\pi}{\alpha} a_n Ai(\xi_n) Gi'(\xi_n) \quad (55)$$

where we have used (71) (see Appendix A), and $Gi(y)$ is a Scorer function.

The T -bond pricing function therefore is given by the following simple formula:

$$v(z, t, T) = e^{-\eta(t, T)} \sum_{n=1}^\infty \frac{\pi Gi'(\xi_n)}{|\xi_n| Ai(\xi_n)} Ai\left(\frac{z - \chi_n(t)}{\beta}\right) e^{-\chi_n(t)(T-t)} \quad (56)$$

where

$$\chi_n(t) = \chi(t) + E_n = \chi(t) + \beta |\xi_n| \quad (57)$$

and $\eta(t, T)$ is defined in (15). Recall that $\beta = (\sigma^2/2)^{1/3}$.

Taking into account the asymptotics given in Appendix A, we see that the series is well-behaved at large n . Thus, let

$$v(z, t, T) \equiv \sum_{n=1}^\infty v_n(z, t, T) \quad (58)$$

For large n such that $|\xi_n| \gg (z - \chi(t))/\beta$, the leading asymptotics are:

$$v_n(z, t, T) \sim u_n \exp(-\gamma(t, T) n^{2/3}) \quad (59)$$

$$u_n \equiv (-1)^{n+1} \sqrt{\frac{2}{3n}} \quad (60)$$

$$\gamma(t, T) \equiv \beta (T - t) \left(\frac{3\pi}{2}\right)^{2/3} \quad (61)$$

So, asymptotically, we have an alternating series, which converges according to the Leibniz criterion.²¹ In numerical computations one would truncate the series at a suitably chosen finite n (see below).

3.3.1 Parameter Count and Model Calibration

Suppose we have data for zero-coupon²² T -bond prices. How many parameters would we need to fit to calibrate (56)? We need to break this down. Let us start with the case of vanishing drift $\nu(t) \equiv 0$. Then the answer is that we have 3 parameters to fit. Indeed, in (56) we have z , β (which is fixed by σ) and r_0 (note that $\chi(t) \equiv r_0$ when $\nu(t) \equiv 0$). However, looking at (5) for this model with $\nu(t) \equiv 0$

$$\partial_t v(z, t, T) + \frac{1}{2} \sigma^2 \partial_z^2 v(z, t, T) - z v(z, t, T) = 0 \quad (62)$$

$$v(z, T, T) = 1 \quad (63)$$

it might appear that we have only 2 parameters, z and σ , to fit. The third parameter, r_0 , is simply the location of the reflecting boundary,²³ which is a free²⁴ parameter. In fact, in the Ho and Lee model, before introducing a reflecting boundary, the spectrum of (62) is continuous.²⁵ Once we introduce a reflecting boundary, the spectrum is discrete and, once again, its nonnegativity does not require that the reflecting boundary be at $r_- = 0$. It suffices to require that $r_- = r_0 \geq -\beta |\xi_1|$.

When the drift $\nu(t)$ is nonzero, we have a choice. Thus, we can try to fit more parameters. *E.g.*, we can assume that $\nu(t) \equiv \nu_0 \neq 0$ is constant; then we have four parameters to fit. Or we can assume that $\nu(t)$ is a general polynomial of degree k , so we have $4 + k$ parameters to fit. Similarly, we can assume that $\nu(t)$ is some function, *e.g.*, $\nu(t) = \nu_0 \cos(\omega t)$, in which case we have five parameters to fit. *Etc.*

Alternatively, we can follow a different procedure, which we set forth here. Instead of trying to fit $\nu(t)$, we can first fit the three parameters z , β and r_0 (*e.g.*, via the least squares method – see below) *assuming* $\nu(t) \equiv 0$, and then attribute the difference between the so-fitted model yield curve $R_m(t, T)$ and the empirical yield curve $R_e(t, T)$ to nontrivial $\nu(t)$. We will refer to this difference as the “residual” yield: $R_r(t, T) \equiv R_e(t, T) - R_m(t, T)$. In fact, looking at (56) it is evident that for nontrivial $\nu(t)$ it is more convenient to fit z (which is nothing but r_t), β and $\chi(t)$ (as opposed to r_0). So, below, after we fit z , β and r_0 in the $\nu(t) \equiv 0$ case, we will use

²¹ Note that $\sum_{n=1}^{\infty} u_n = \sqrt{2/3} (1 - \sqrt{2}) \zeta(1/2) \approx 0.494$, where $\zeta(s)$ is the Riemann zeta function.

²² In practice, unless the yield data is readily available, we may have data for coupon-bearing bond prices, which then are bootstrapped to obtain zero-coupon bond prices.

²³ When $\nu(t) \equiv 0$, the reflecting boundary at $x_- = 0$ for the Brownian motion process W_t translates into a reflecting boundary at $r_- = r_0$ for the short-rate process r_t . As discussed in more detail in Appendix B, this is no longer the case for a general time-dependent drift $\nu(t)$.

²⁴ Modulo the requirement (22), that is (see below). Note that $\chi_*(t) \equiv 0$ when $\nu(t) \equiv 0$.

²⁵ Moreover, (62) has a symmetry under the transformation $v(z, t, T) \rightarrow e^{-\zeta t} v(z + \zeta, t, T) \equiv \tilde{v}_\zeta(z, t, T)$, where ζ is an arbitrary constant. *I.e.*, if $v(z, t, T)$ satisfies (62) and (63), then so does $\tilde{v}_\zeta(z, t, T)$ for arbitrary ζ .

the so-obtained r_0 as $\chi(t)$ in the nontrivial $\nu(t)$ case.²⁶ Then we have the following simple formula for the “residual” yield:

$$R_r(t, T) = \frac{\eta(t, T)}{T - t} \quad (64)$$

so we can read $\eta(t, T)$ off the empirical yield curve once we fit $R_m(t, T)$, which will give us approximate²⁷ shapes of $\chi(s)$ and $\nu(s)$ for $t \leq s \leq T$.

3.3.2 An Illustrative Example: Japanese Government Bonds

For illustrative and comparison purposes, we have used the zero-coupon T -bond pricing formula (56)²⁸ in the Ho and Lee model on a semi-infinite line with $\nu(t) \equiv 0$ (“Model-2”) to fit the Japanese Government Bond data used in (Gorovoi and Linetsky, 2004) to calibrate Black’s model of interest rates as options (Black, 1995)²⁹ with the underlying “shadow rate” following the Vasicek model (“Model-1”). As in (Gorovoi and Linetsky, 2004), we fit the model by minimizing the root mean squared error (RMSE) between the empirical yield curve (Table 1, column 4) and the Model-2 yield curve (see above).

Table 1 summarizes our results. The calibrated model parameters in Model-2 are³⁰ $z \approx -0.00184$, $\beta \approx 0.0924$ (which implies $\sigma \approx 0.0397$), $r_0 \approx -0.05834$. This implies that the initial short-rate value $r_t = z$ (here $t = 02/03/2002$) is essentially 0 (within the 2-digit precision of the underlying bootstrapped yield data in column 4 of Table 1). On the other hand, in Model-2 the lower bound on the short-rate process is $r_- = r_0 \approx -5.834\%$, which is close to the initial value -5.12% of the “shadow rate” found in (Gorovoi and Linetsky, 2004) for Model-1. However, due to the discrete spectrum in Model-2, the fact that r_- is negative is not particularly informative. The short-rate modes that contribute into the bond (and other) prices are given by $\chi_n = r_0 + E_n$ (recall that in this case $\chi(t) = r_0$, so $\chi_n(t)$ are constant), which are positive in this model. The first ten values of χ_n are given in column 1, Table 3. It is clear that at long maturities only a few lowest-lying levels have significant contributions into (56). However, at short maturities a significant number of levels must be included.³¹

The Model-2 and empirical yields are plotted in Figure 1. The fit in Model-2, which has fewer (to wit, 3) parameters than Model-1,³² is actually better than in

²⁶ Equivalently, we can simply set $t = 0$, so $\chi(t) = r_0$.

²⁷ Typically, there are not that many maturities available, so reconstructing $\chi(s) = \partial_s \eta(t, s) + \chi(t)$ and $\nu(s) = \dot{\chi}(s)$ would involve piecewise polynomial splines.

²⁸ The Airy functions $Ai(y)$ and $Bi(y)$ and their zeroes are built-in within the “gsl” package in R. Their integrals are not, so we evaluated them (see (76), Appendix A).

²⁹ A similar model was independently discussed by Rogers (1995).

³⁰ All dimensionful parameters are quoted in the units of 1 year. Note that r_t , r_0 , z , β and E_n have dimension (time)⁻¹, σ has dimension (time)^{-3/2}, and W_t has dimension (time)^{1/2}.

³¹ In our computation it was (more than) sufficient to truncate the series in (56) at $n = 300$.

³² In Model-1 the underlying “shadow rate” process X_t follows the Vasicek model (6) with

Model-1. The RMSE between the empirical yield curve (Table 1, column 4) and the Model-1 yield curve (Table 1, column 5) $\text{RMSE}(\text{Model-1}) \approx 6.37 \times 10^{-4}$. The RMSE between the empirical yield curve and the Model-2 yield curve (Table 1, column 6) $\text{RMSE}(\text{Model-2}) \approx 5.91 \times 10^{-4}$. This implies that the mean-reverting feature in Model-1 (which introduces two additional parameters) apparently does not improve the fit. We have also computed a straightforward (not piecewise spline) cubic fit with the intercept, which amounts to fitting a general cubic polynomial into the empirical yield curve using a linear model. The RMSE between the empirical yield curve and the cubic fit yield curve (Table 1, column 7) $\text{RMSE}(\text{Cubic}) \approx 6.60 \times 10^{-4}$. From Table 1, column 7 it is evident that both Model-1 and Model-2 are significantly better than the cubic fit. The cubic fit works very well at long maturities, but fails badly at short maturities. This is not surprising considering that, as mentioned above, at long maturities only the lowest few modes contribute, whereas at short maturities a large number of modes do. Furthermore, this suggests that a good model fit (both for Model-1 and Model-2) may not be a universal feature and may not persist to other data, in which case the “residual” yield might have to be attributed to nontrivial drift. The “residual” drift in Model-2 is plotted in Figure 2.

3.3.3 An Illustrative Example: Recent US Treasury Yield Curve

Table 2 summarizes the Model-2 fit for a recent US Treasury yield curve. The calibration procedure is the same as above. Column 3 of Table 2 corresponds to the Model-2 fit based on all maturities T ; the empirical and Model-2 yields are plotted in Figure 3, and the “residual” yield is plotted in Figure 4; the first 10 values of the χ_n spectrum are given in Table 3, column 2. Column 4 of Table 2 corresponds to the Model-2 fit based only on the maturities $T \geq 1$ yr; the empirical and Model-2 yields are plotted in Figure 5, and the “residual” yield is plotted in Figure 6; the first 10 values of the χ_n spectrum are given in Table 3, column 3. For comparison purposes, columns 5 and 6 of Table 2 contain straightforward cubic fits into the empirical data for all maturities and $T \geq 1$ yr maturities only, respectively. We have the following RMSE for the above fits: $\text{RMSE}(\text{Model-2, All } T) \approx 1.99 \times 10^{-3}$; $\text{RMSE}(\text{Model-2, } T \geq 1 \text{ yr}) \approx 4.91 \times 10^{-4}$; $\text{RMSE}(\text{Cubic, All } T) \approx 5.07 \times 10^{-4}$; $\text{RMSE}(\text{Cubic, } T \geq 1 \text{ yr}) \approx 5.39 \times 10^{-4}$. The Model-2 fit, which assumes vanishing drift, is better than the cubic fit for longer maturities, but not for shorter ones.

Looking at the results it is clear that Model-2 provides a very good fit for maturities $T \geq 1$ yr, but not for short maturities $T < 1$ yr. For these short maturities, the “residual” yield attributed to nontrivial drift is large and cannot be neglected. Moreover, apparently, the drift is not even approximately constant – for a constant drift $\nu(t) \equiv \nu_0$ we would have the “residual” yield of the form $R_r(t, T) = (\nu_0/2)(T - t)$. So, the drift appears to have nontrivial time dependence.

constant σ , θ and α , which together with $z = r_t$ give 4 parameters. The fifth parameter is the location of the sewing point r_- , *i.e.*, $r_t = r_- + (X_t)^+$. In (Gorovoi and Linetsky, 2004) it is set to zero, $r_- = 0$. However, here too the spectrum can be nonnegative for a range of $r_- < 0$.

3.4 Bond Pricing on an Interval

For the sake of completeness, let us briefly discuss zero-coupon T -Bond pricing in the Ho and Lee model on an interval. We have

$$c_n = \int_0^L dx \psi_n(x) = \frac{\pi}{\alpha} a_n [\phi_n(0) Gi'(-e_n) - \phi_n(L) Gi'(\alpha L - e_n)] \quad (65)$$

where we have used (71) and (72) (see Appendix A), and $\phi_n(x)$ is defined in (47).

The T -bond pricing function therefore is given by the following simple formula:

$$v(z, t, T) = e^{-\eta(t, T)} \sum_{n=1}^{\infty} b_n \phi_n \left(\frac{z - \chi(t)}{\sigma} \right) e^{-\chi_n(t)(T-t)} \quad (66)$$

$$b_n \equiv \pi \frac{\phi_n(0) Gi'(-e_n) - \phi_n(L) Gi'(\alpha L - e_n)}{e_n \phi_n^2(0) + (\alpha L - e_n) \phi_n^2(L)} \quad (67)$$

where $\chi_n(t) = \chi(t) + E_n = \chi(t) + \beta e_n$, and $e_n > 0$ are the roots of (49). Recall that $\alpha \equiv (2\sigma)^{1/3}$ and $\beta \equiv (\sigma^2/2)^{1/3}$. If we assume vanishing drift, then the Ho and Lee model on an interval has four parameters to fit: z , σ , r_0 (the lower reflecting barrier is at $r_- = r_0$) and L (the upper reflecting barrier is at $r_+ = r_0 + L$). The calibration can be done as above with the caveat that numerical estimations involving the Airy function $Bi(y)$ are trickier as $Bi(y)$ diverges for large positive y (see Appendix A for some useful formulas).

4 Concluding Remarks

The condition (22) restricts the allowed drifts $\nu(t)$. As mentioned above, the l.h.s. of this condition should be some positive number, which we will denote by R_{min} . Then we have³³

$$\chi_*(t) + \chi(t) + E_1 \geq R_{min} \quad (68)$$

Let us now consider constant drift $\nu(t) \equiv \nu$. We have $\chi(t) = r_0 + \nu t$, so $\eta(t, T) = \nu(T-t)^2/2$ and $\chi_*(t)$ is $+\infty$ if $\nu > 0$ and $-\infty$ if $\nu < 0$. This implies that constant negative drift is not allowed.³⁴ This is evident from the fact that when the drift is constant we have $r_t = V(W_t) + \nu t$. In fact, positive constant ν is not realistic either because it would drive r_t to large values. A reasonable assumption then is that $\chi_*(t)$ should be finite, which implies that

$$\lim_{s \rightarrow \infty} |\chi(s)| \leq \tilde{\chi} \quad (69)$$

where $\tilde{\chi}$ is finite.

³³ This holds for general $r_t = V(W_t) + \chi(t)$. If $V(x)$ is confining (e.g., $V(x) = \omega^2 x^2/2$), then there is no need for a reflecting boundary as the spectrum is discrete and bounded from below.

³⁴ In the solution (90) corresponding to introducing a reflecting barrier for r_t (as opposed to W_t) constant negative drift *a priori* is allowed as r_t is reflected when it hits its lower boundary r_* .

Another point worth commenting on is that, while for time-homogeneous cases (*i.e.*, for time-independent parameters) we can consider “option-like” models with $r_t = (X_t)^+$ and the underlying “shadow” rate X_t following processes such as Vasicek, CIR, *etc.*, which have discrete spectra, X_t cannot follow the Ho and Lee model as the latter has continuous spectrum.³⁵ In contrast, we can have a reflecting barrier in the Ho and Lee model. Such a barrier can be introduced for W_t for a time-dependent drift (subject to the above conditions), and also on r_t for constant drift, which is negative in the case with only the lower barrier, but can be positive in the case where both lower and upper barriers are present. However, constant drift is limited in its applicability as can be seen from the U.S. Treasury data we discussed above.

A Some Properties of Airy and Scorer Functions

In this appendix we collect some properties of the Airy and Scorer functions used in the main text. Unless stated otherwise, these properties are taken from (Abramowitz and Stegun, 1964).

- Integral identity:

$$\int dy f_1(y) f_2(y) = y f_1(y) f_2(y) - f_1'(y) f_2'(y) \quad (70)$$

where each f_1 and f_2 can be either $Ai(y)$ or $Bi(y)$. Eq. (70) can be obtained via integration by parts and using the Airy equation $f_i''(y) = y f_i(y)$, $i = 1, 2$.

- Integral identities:

$$\frac{1}{\pi} \int_y^\infty dw Ai(w) = Ai(y) Gi'(y) - Ai'(y) Gi(y) \quad (71)$$

$$\frac{1}{\pi} \int_0^y dw Bi(w) = Bi'(y) Gi(y) - Bi(y) Gi'(y) \quad (72)$$

$$\int_0^\infty dw Ai(w) = \frac{1}{3} \quad (73)$$

where $Gi(y)$ is a Scorer function. Let

$$\mathcal{A}(-y) \equiv \int_{-y}^0 dw Ai(w) \quad (74)$$

$$\mathcal{B}(-y) \equiv \int_{-y}^0 dw Bi(w) \quad (75)$$

where $y > 0$. The integrals $\mathcal{A}(-y)$ and $\mathcal{B}(-y)$ can be evaluated numerically. It follows from (73) that

$$\int_{-y}^\infty dw A(w) = \frac{1}{3} + \mathcal{A}(-y) \quad (76)$$

³⁵ Here one can wonder if it would make sense to consider “option-like” models for W_t . However, if we replace W_t by $(W_t)^+$ in $r_t = V(W_t) + \chi(t)$, the spectrum will be continuous.

where $y > 0$. It further follows from (71) and (72) that

$$\pi Gi'(-y) = \frac{[\frac{1}{3} + \mathcal{A}(-y)] Bi'(-y) - \mathcal{B}(-y) Ai'(-y)}{Ai(-y) Bi'(-y) - Bi(-y) Ai'(-y)} \quad (77)$$

which allows to evaluate $Gi'(-y)$ numerically for $y > 0$. In some cases, the integral representation for $Gi(y > 0)$ given in (Gil, Segura and Temme, 2001) may be useful for evaluating $Gi'(y > 0)$.

- Leading asymptotic behavior

$$Ai(-y) \sim \frac{y^{-1/4}}{\sqrt{\pi}} \sin\left(\frac{2}{3} y^{3/2} + \frac{\pi}{4}\right) \quad (78)$$

$$Gi'(-y) \sim \frac{y^{1/4}}{\sqrt{\pi}} \sin\left(\frac{2}{3} y^{3/2} + \frac{\pi}{4}\right) \quad (79)$$

at $y \gg 1$.

- Leading asymptotic behavior at large n :

$$\xi_n \sim -\left(\frac{3\pi}{8} [4n - 3]\right)^{2/3} \quad (80)$$

$$Ai(\xi_n) \sim \frac{(-1)^{n+1}}{\sqrt{\pi}} |\xi_n|^{-1/6} \quad (81)$$

$$Gi'(\xi_n) \sim \frac{(-1)^{n+1}}{\sqrt{\pi}} |\xi_n|^{1/6} \quad (82)$$

where ξ_n ($0 > \xi_1 > \xi_2 > \dots$) are the zeros of $Ai'(y)$.

B Reflecting Barriers for the Short-rate Process

In this section we discuss the issues associated with introducing reflecting boundaries directly for the short-rate process r_t as opposed to the underlying Brownian motion process W_t . Our starting point is (5) together with the terminal condition $v(z, T, T) = \tilde{Y}(z)$. When $\sigma(r_t, t)$ and $\nu(r_t, t)$ have no explicit time dependence, reflecting barriers for r_t can be introduced as in, *e.g.*, (Goldstein and Keirstead, 1997) and (Gorovoi and Linetsky, 2004).³⁶ Even if $\sigma(r_t, t)$ has no explicit time dependence, for general, explicitly time-dependent $\nu(r_t, t)$ things are trickier. In fact, for our purposes here, to illustrate our main point, it will suffice to consider the case where $\sigma(r_t, t) \equiv \sigma$ is constant and $\nu(r_t, t) \equiv \nu(t)$ is independent of r_t , but is a deterministic function of t . Eq. (5) then reduces to

$$\nu(t) \partial_z v(z, t, T) + \partial_t v(z, t, T) + \frac{1}{2} \sigma^2 \partial_z^2 v(z, t, T) - z v(z, t, T) = 0 \quad (83)$$

³⁶ In this case, (5) can be transformed into the Schrödinger equation with time-independent potential (a.k.a. Liouville normal form) via a Liouville transformation.

An analogue of the Liouville transformation in this case is

$$v(z, t, T) \equiv \exp\left(-\frac{\nu(t)}{\sigma^2} z\right) u(z, t, T) \quad (84)$$

Then the PDE for $u(z, t, T)$ reads:

$$\partial_t u(z, t, T) + \frac{1}{2}\sigma^2 \partial_z^2 u(z, t, T) - \left[z \left(1 + \frac{\dot{\nu}(t)}{\sigma^2} \right) + \frac{\nu^2(t)}{2\sigma^2} \right] u(z, t, T) = 0 \quad (85)$$

This is the Schrödinger equation with time-dependent potential – unless $\nu(t)$ is constant, that is. When $\nu(t)$ is a linear function of t so that $\dot{\nu}(t) \equiv \rho$ is constant, the potential is time-dependent but factorized, so in this special case the solution to (85) is given by

$$u(z, t, T) = \exp\left(\int_0^t ds \frac{\nu^2(s)}{2\sigma^2}\right) w(z, t, T) \quad (86)$$

where $w(z, t, T)$ solves the following Schrödinger equation with a linear potential:

$$\partial_t w(z, t, T) + \frac{1}{2}\sigma^2 \partial_z^2 w(z, t, T) - z \left(1 + \frac{\rho}{\sigma^2} \right) w(z, t, T) = 0 \quad (87)$$

which can be solved as in the main text; provided, however, that the boundary condition can be consistently specified.

This is where a difficulty arises irrespective of whether $\nu(t)$ is a linear function of t or not – so long as it is not constant, that is. Thus, if we impose a reflecting (Neumann) boundary condition for some $r_t = r_*$

$$\partial_z v(z, t, T)|_{z=r_*} = 0 \quad (88)$$

then for $u(z, t, T)$ we have the following Robin boundary condition:

$$\partial_z u(z, t, T)|_{z=r_*} = \frac{\nu(t)}{\sigma^2} u(z, t, T) \Big|_{z=r_*} \quad (89)$$

For constant $\nu(t)$ we can perform the separation of variables. However, even for linear $\nu(t)$ the straightforward separation of variables procedure cannot be applied and the problem becomes more difficult to solve.

Let us briefly outline the solution for constant $\nu(t) \equiv \nu$, primarily to illustrate the difference with the corresponding solution in the case of a reflecting boundary for the underlying Brownian motion we discuss in the main text. We have³⁷

$$v(z, t, T) = \psi(z/\beta, T - t) \quad (90)$$

$$\psi(y, \tau) = e^{-\gamma y} \sum_{n=1}^{\infty} d_n Ai(y - e_n) e^{-\lambda_n \tau} \quad (91)$$

³⁷ Here we focus on the solution with only one (lower) boundary. The solution with both (lower and upper) boundaries can also be readily constructed and involves both $Ai(y)$ and $Bi(y)$.

where $\lambda_n \equiv \beta(\gamma^2 + e_n)$, $\beta \equiv (\sigma^2/2)^{1/3}$, $\gamma \equiv \nu/(2\sigma^4)^{1/3}$, and e_n are the roots of the equation

$$Ai'(y_* - e_n) = \gamma Ai(y_* - e_n) \quad (92)$$

which is a consequence of the boundary condition (89) corresponding to a reflecting boundary³⁸ at $r_t = r_*$, and $y_* \equiv r_*/\beta$. The coefficients d_n are fixed via the terminal condition $v(z, T, T) = \tilde{Y}(z)$. For a zero-coupon T -bond we have $\tilde{Y}(z) \equiv 1$ and

$$d_n = \frac{\int_{y_*}^{\infty} dy e^{\gamma y} Ai(y - e_n)}{\int_{y_*}^{\infty} dy [Ai(y - e_n)]^2} = e^{\gamma e_n} \frac{I(\gamma, e_n - y_*) + \tilde{I}(\gamma)}{(e_n - y_* - \gamma^2) [Ai(y_* - e_n)]^2} \quad (93)$$

$$I(\gamma, y) \equiv \int_{-y}^0 dw e^{\gamma w} Ai(w) \quad (94)$$

$$\begin{aligned} \tilde{I}(\gamma) &\equiv \int_0^{\infty} dw e^{\gamma w} Ai(w) = \\ &e^{\gamma^3/3} \left[\frac{1}{3} + \frac{{}_1F_1\left(\frac{1}{3}; \frac{4}{3}; -\frac{\gamma^3}{3}\right) \gamma}{3^{4/3} \Gamma(4/3)} - \frac{{}_1F_1\left(\frac{2}{3}; \frac{5}{3}; -\frac{\gamma^3}{3}\right) \gamma^2}{3^{5/3} \Gamma(5/3)} \right] \end{aligned} \quad (95)$$

where $\Gamma(y)$ is the Gamma function, and ${}_1F_1(a; b; y)$ is a generalized hypergeometric function. In (95) we have used a Laplace transform of the Airy function $Ai(y)$, see Eq. (9.10.14) in (DLMF, 2015). In practice, if $|\gamma|$ is not large, then the integral $\tilde{I}(\gamma)$ can be evaluated by truncating the series

$$\tilde{I}(\gamma) = \frac{1}{3} \sum_{n=0}^{\infty} \frac{(\gamma/3^{1/3})^n}{\Gamma(n/3 + 1)} \quad (96)$$

which follows from the Mellin transform of $Ai(y)$, see Eq. (9.10.17) in (DLMF, 2015). Asymptotically, this series behaves as the Taylor expansion of $(1/3) \exp(\gamma^3/3)$.

Acknowledgments

I would like to thank Eyal Neuman for discussions on Brownian motion with reflecting barriers, which prompted me to think about this topic.

References

- [1] Abramowitz, M. and Stegun, I.A. (eds.) (1964) *Handbook of Mathematical Functions with Formulas, Graphs, and Mathematical Tables*. New York, NY: Dover Publications.
- [2] Ait-Sahalia, Y. (1996) Testing continuous-time models of the spot interest rate. *Review of Financial Studies* 9(2): 385-426.

³⁸ The reflecting boundary in (Goldstein and Keirstead, 1997) was set at $r_* = 0$.

- [3] Antonov, A. and Spector, M. (2011) General Short-Rate Analytics. *Risk Magazine*, May 2011: 66-71.
- [4] Bakshi, G. and Chen, W. (1996) Inflation, asset prices and the term structure of interest rates in monetary economies. *Review of Financial Studies* 9(1): 241-275.
- [5] Beaglehole, D. and Tenney, M. (1991) General solutions of some interest rate-contingent claim pricing equations. *Journal of Fixed Income* 1(2): 69-83.
- [6] Black, F. (1995) Interest Rates as Options. *J. Finance* 50(5): 1371-1376.
- [7] Black, F., Derman, E. and Toy, W. (1990) A One-Factor Model of Interest Rates and Its Application to Treasury Bond Options. *Financial Analysts Journal* 46(1): 33-39.
- [8] Black, F. and Karasinski, P. (1991) Bond and Option Pricing when Short Rates are Lognormal. *Financial Analysts Journal* 47(4): 52-59.
- [9] Brennan, M.J. and Schwartz, E.S. (1979) A Continuous Time Approach to the Pricing of Bonds. *Journal of Banking and Finance* 3(2): 133-155.
- [10] Carr, P., Ellis, K. and Gupta, V. (1998) Static hedging of exotic options. *The Journal of Finance* 53(3): 1165-1190.
- [11] Carr, P. and Jarrow, R. (1990) The Stop-Loss Start-Gain Paradox and Option Valuation: A New Decomposition into Intrinsic and Time Value *Rev. Financial Stud.* 3(3): 469-492.
- [12] Carr, P. and Linetsky, V. (2000) The Valuation of Executive Stock Options in an Intensity-Based Framework. *European Finance Rev.* 4(3): 211-230.
- [13] Cox, J.C., Ingersoll, J.E. and Ross, S.A. (1985) A theory of term structure of interest rates. *Econometrica* 53(2): 385-407.
- [14] Conley, T., Hansen, L.P., Luttmer, E.G.J. and Scheinkman, J. (1997) Short-Term Interest Rates as Subordinated Diffusions. *Rev. Financial Stud.* 10(3): 525-577.
- [15] Constantinides, G.M. (1992) A theory of the nominal term structure of interest rates. *Rev. Financial Stud.* 5(4): 531-552.
- [16] Dai, Q. and Singleton, K. (2000) Specification Analysis of Affine Term Structure Models. *J. Finance* 55(5): 1943-1978.
- [17] DLMF (2015) Digital Library of Mathematical Functions. National Institute of Standards and Technology. <http://dlmf.nist.gov/>.

- [18] Duffie, D., and Kan, R. (1996) A Yield Factor Model of Interest Rates. *Math. Finance* 6(4): 379-406.
- [19] Gil, A., Segura, J. and Temme, N.M. (2001) On nonoscillating integrals for computing inhomogeneous Airy functions. *Math. Comp.* 70(235): 1183-1194; arXiv:math/0109187 [math.NA].
- [20] Goldstein, R.S. and Keirstead, W.P. (1997) On the Term Structure of Interest Rates in the Presence of Reflecting and Absorbing Boundaries. SSRN Working Paper, <http://ssrn.com/abstract=19840>.
- [21] Gorovoi, V. and Linetsky, V. (2004) Black's Model of Interest Rates as Options, Eigenfunction Expansions and Japanese Interest Rates. *Mathematical Finance* 14(1): 49-78.
- [22] Heath, D., Jarrow, R. and Morton, A. (1992) Bond Pricing and the Term Structure of Interest Rates: A New Methodology for Contingent Claims Valuation. *Econometrica* 60(1): 77-105.
- [23] Ho, S.Y. and Lee, S.-B. (1986) Term Structure Movements and Pricing Interest Rate Contingent Claims. *Journal of Finance* 41(5): 1011-1029.
- [24] Hull, J. and White, A. (1990) Pricing interest rate derivative securities. *The Review of Financial Studies* 3(4): 573-592.
- [25] Jamshidian, F. (1989) An Exact Bond Option Pricing Formula. *J. Finance* 44(1): 205-209.
- [26] Kakushadze, Z. (2014) Path Integral and Asset Pricing. *Quantitative Finance* (forthcoming); SSRN Accepted Paper, <http://ssrn.com/abstract=2506430>.
- [27] Kalotay, A.J., Williams, G.O. and Fabozzi, F.J. (1993) A Model for Valuing Bonds and Embedded Options. *Financial Analysts Journal* 49(3): 35-46.
- [28] Krugman, P.R. (1991) Target Zones and Exchange Rate Dynamics. *The Quarterly Journal of Economics* 106(3): 669-682.
- [29] Leippold, M. and Wiener, Z. (2004) Efficient Calibration of Trinomial Trees for One-Factor Short Rate Models. *Review of Derivatives Research* 7(3): 213-239.
- [30] Lewis, A.L. (1998) Applications of Eigenfunction Expansions in Continuous-Time Finance, *Math. Finance* 8(4): 349-383.
- [31] Lim, N. and Privault, N. (2014) Analytic bond pricing for short rate dynamics evolving on matrix Lie groups. Preprint.
<http://www.ntu.edu.sg/home/nprivault/papers/matrix%5Flie%5Fgroups.pdf>.

- [32] Linetsky, V. (2005) On the Transition Densities for Reflected Diffusions. *Adv. App. Prob.* 37(2): 435-460.
- [33] Longstaff, F.A. (1989) A Nonlinear General Equilibrium Model of the Term Structure of Interest Rates. *Journal of Financial Economics* 23(2): 195-224.
- [34] Longstaff, F.A. and Schwartz, E.S. (1992) Interest Rate Volatility and the Term Structure: A Two-Factor General Equilibrium Model. *Journal of Finance* 47(4): 1259-82.
- [35] Lucas, R. (1978) Asset Prices in an Exchange Economy. *Econometrica* 46(6): 1429-1445.
- [36] Merton, R.C. (1973) Theory of Rational Option Pricing. *Bell Journal of Economics and Management Science* 4(1): 141-183.
- [37] Park, F.C., Chun, C.M., Han, C.W. and Weber, N. (2011) Interest rate models on Lie groups. *Quantitative Finance* 11(4): 559-572.
- [38] Rendleman, R. and Bartter, B. (1980) The Pricing of Options on Debt Securities. *Journal of Financial and Quantitative Analysis* 15(1): 11-24.
- [39] Rogers, L.C.G. (1995) Which Model for Term-Structure of Interest Rates Should One Use? In: Davis, M.H.A., Duffie, D. and Karatzas, I. (eds.) *Proceedings of IMA Workshop on Mathematical Finance*, IMA Vol. 65. New York, NY: Springer-Verlag, pp. 93-116.
- [40] Rogers, L.C.G. (1996) Gaussian Errors. *Risk* 9(1): 42-45.
- [41] Stehlíková, B. and Capriotti, L. (2014) An Effective Approximation for Zero-Coupon Bonds and Arrow-Debreu Prices in the Black-Karasinski Model. *International Journal of Theoretical and Applied Finance* 17(6): 1450037.
- [42] Tourrucôo, F., Hagan P.S. and Schleiniger, G.F. (2007) Approximate Formulas for Zero-Coupon Bonds. *Applied Mathematical Finance* 14(3): 107-226.
- [43] Ueno, Y., Baba, N. and Sakurai, Y. (2006) The Use of the Black Model of Interest Rates as Options for Monitoring the JGB Market Expectations. Bank of Japan Working Paper Series, No.06-E-15.
- [44] Uhlenbeck, G.E. and Ornstein, L.S. (1930) On the theory of Brownian motion. *Phys. Rev.* 36: 823-841.
- [45] U.S. Treasury (2015) <http://www.treasury.gov>, accessed January 29, 2015.
- [46] Vasicek, O.A. (1977) An equilibrium characterization of the term structure. *Journal of Financial Economics* 5(2): 177-188.

Table 1: The calibration results for the zero-coupon T -bond pricing formula (56) in the Ho and Lee model on a semi-infinite line with vanishing drift (“Model-2”). The first five columns are taken from (Gorovoi and Linetsky, 2004). The first three columns give the Bloomberg data as of $t = 02/03/2002$ for the Japanese Government Bonds: coupon, maturity T and price. The fourth column gives the corresponding bootstrapped zero-coupon bond yields. The fifth column gives the calibrated model yields calculated in (Gorovoi and Linetsky, 2004) for Black’s model of interest rates as options (Black, 1995) with the underlying “shadow rate” following the Vasicek model (“Model-1”). The sixth column gives calibrated model yields we calculated based (56). The calibrated model parameters are $z \approx -0.00184$, $\beta \approx 0.0924$ (which implies $\sigma \approx 0.0397$), $r_0 \approx -0.05834$. For illustrative purposes we have kept 3 digits in the sixth column. In the seventh column we have included the yield curve from fitting a general cubic polynomial into the empirical data in the fourth column.

Coupon	Maturity	Price	Empirical 0-Coupon Yield (%)	Model-1 Yield (%)	Model-2 Yield (%)	Cubic Fit Yield (%)
4.2	3/20/2003	104.648	0.02	0.03	0.023	-0.106
3.4	3/22/2004	106.900	0.14	0.17	0.106	0.156
4.4	3/21/2005	112.729	0.30	0.36	0.338	0.395
3.1	3/20/2006	110.481	0.54	0.57	0.571	0.615
2.6	3/20/2007	109.326	0.76	0.78	0.788	0.818
1.9	3/20/2008	105.578	0.98	0.98	0.988	1.005
1.9	3/20/2009	104.723	1.24	1.16	1.169	1.175
1.7	3/22/2010	102.521	1.40	1.33	1.333	1.331
1.4	3/21/2011	99.314	1.51	1.48	1.481	1.472
1.5	12/20/2011	99.997	1.53	1.59	1.584	1.569
3.8	9/20/2016	123.287	2.11	2.09	2.084	2.040
2.1	12/20/2021	98.411	2.29	2.44	2.434	2.360
2.4	11/20/2031	94.810	2.88	2.79	2.801	2.869

Table 2: The calibration results for the zero-coupon T -bond pricing formula (56) in the Ho and Lee model on a semi-infinite line with vanishing drift (“Model-2”). The first two columns are taken from the U.S. Treasury website (U.S. Treasury, 2015) as of $t = 01/29/2015$: maturity T and empirical yield $R_e(t, T)$. The third column is the Model-2 fit including all maturities, for which the calibrated model parameters are $z \approx -0.0027$, $\beta \approx 0.2516$ (which implies $\sigma \approx 0.1785$), $r_0 \approx -0.23163$. The fourth column is the Model-2 fit including only the maturities of 1 year and longer, for which the calibrated model parameters are $z \approx 0.0012$, $\beta \approx 0.2085$ (which implies $\sigma \approx 0.1346$), $r_0 \approx -0.1879$. For illustrative purposes we have kept 3 digits in the third and fourth columns. In the fifth (all maturities) and sixths (only the maturities of 1 year and longer) columns we have included the yield curve from fitting a general cubic polynomial into the empirical data in the second column.

Maturity T	Empirical Yield (%)	Model-2 Yield (%) (All T)	Model-2 Yield (%) ($T \geq 1$ yr)	Cubic Fit Yield (%) (All T)	Cubic Fit Yield (%) ($T \geq 1$ yr)
1 mo	0.01	0.046	—	-0.040	—
3 mo	0.03	0.524	—	0.016	—
6 mo	0.07	-0.005	—	0.097	—
1 yr	0.17	-0.151	0.209	0.252	0.224
2 yrs	0.51	0.292	0.464	0.539	0.521
3 yrs	0.84	0.733	0.797	0.795	0.785
5 yrs	1.28	1.314	1.295	1.221	1.224
7 yrs	1.59	1.629	1.594	1.544	1.554
10 yrs	1.77	1.880	1.845	1.865	1.878
20 yrs	2.11	2.175	2.147	2.086	2.078
30 yrs	2.33	2.273	2.249	2.335	2.336

Table 3: The first 10 values χ_n contributing to the zero-coupon T -bond pricing formula (56) in the Ho and Lee model on a semi-infinite line with vanishing drift (“Model-2”). The first column corresponds to the Japanese Government Bond data in Table 1 (JGB). The second column corresponds to the US Treasury yield data for the fit including all maturities in column 3 of Table 2 (UST1). The third column corresponds to the US Treasury yield data for the fit including only the maturities of 1 year and longer in column 4 of Table 2 (UST2). Note that χ_n are independent of t when the drift vanishes.

χ_n	JGB (%)	UST1 (%)	UST2 (%)
χ_1	3.578	2.470	2.451
χ_2	24.187	58.562	48.934
χ_3	38.718	98.111	81.708
χ_4	51.134	131.906	109.714
χ_5	62.309	162.321	134.919
χ_6	72.628	190.407	158.194
χ_7	82.306	216.749	180.023
χ_8	91.478	241.713	200.711
χ_9	100.236	265.549	220.464
χ_{10}	108.646	288.438	239.432

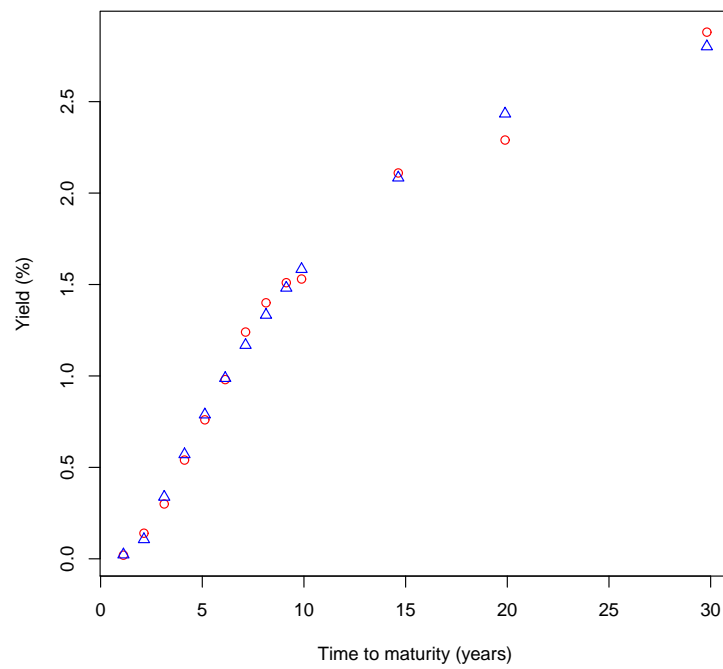


Figure 1. Empirical (circles) and Model-2 (triangles) yield curves corresponding to the data in Table 1.

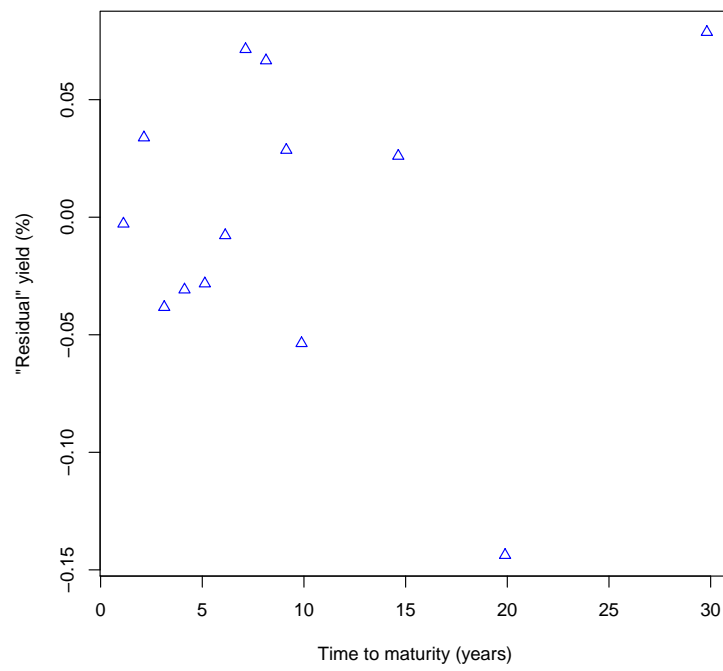


Figure 2. The “residual” yield attributed to nontrivial drift in Model-2 corresponding to the data in Table 1.

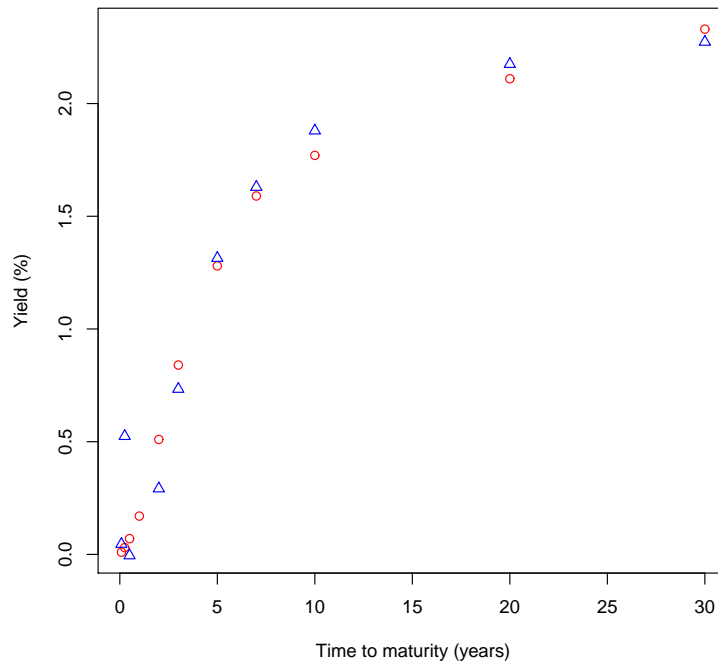


Figure 3. Empirical (circles) and Model-2 (triangles) yield curves corresponding to the data in Table 2 for all maturities.

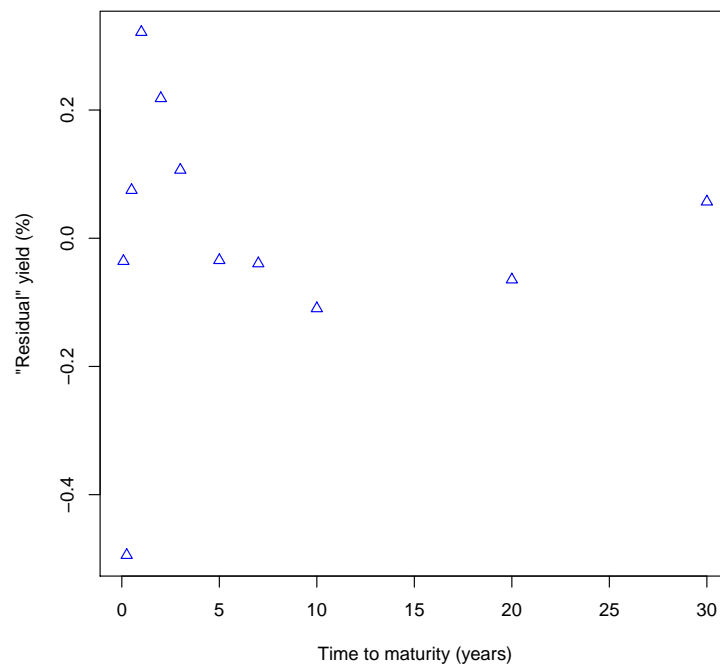


Figure 4. The “residual” yield attributed to nontrivial drift in Model-2 corresponding to the data in Table 2 for all maturities.

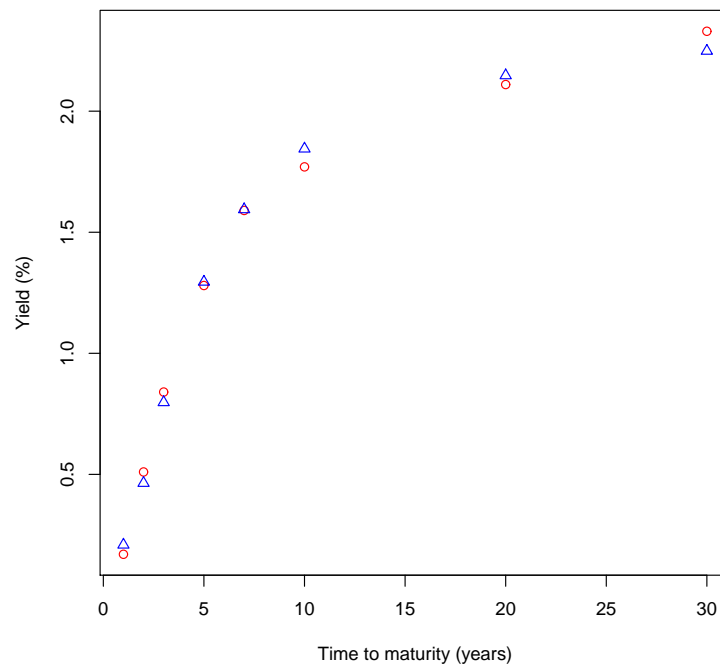


Figure 5. Empirical (circles) and Model-2 (triangles) yield curves corresponding to the data in Table 2 for the maturities of 1 year and longer.

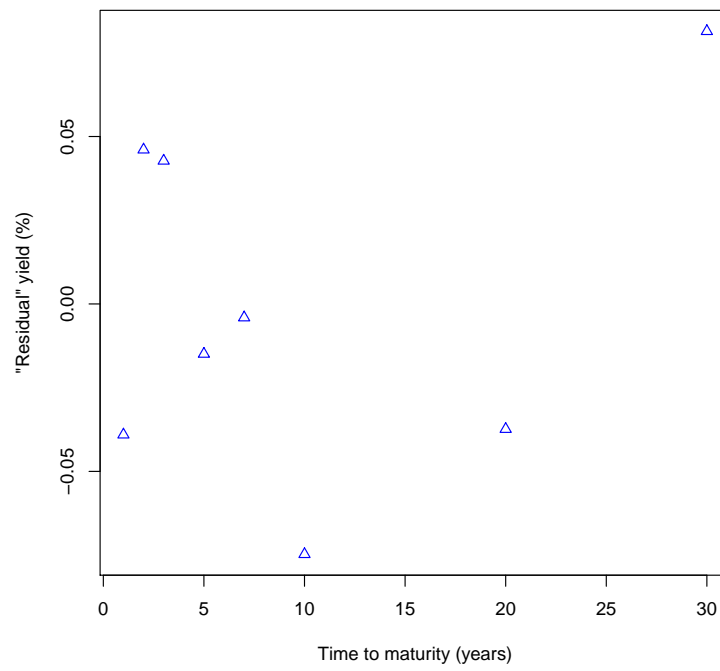


Figure 6. The “residual” yield attributed to nontrivial drift in Model-2 corresponding to data in Table 2 for the maturities of 1 year and longer.